The optimal controller parametric synthesis using variational calculus for a dynamic system general mathematical model

Victoria Vysotska[1,†], Vasyl Lytvyn[1,†], Serhii Vladov[2,*,†], Viktor Vasylenko[3,†] and Oleksii Kryshan[4,†]

[1] *Lviv Polytechnic National University, Stepan Bandera Street 12 79013 Lviv, Ukraine*

[2] *Kremenchuk Flight College of Kharkiv National University of Internal Affairs, Peremohy Street 17/6 39605 Kremenchuk, Ukraine*

[3] *Kharkiv National University of Internal Affairs, L. Landau Avenue 27 61080 Kharkiv, Ukraine*

[4] *Interregional Academy of Personnel Management, Frometivska Street 2 03039 Kyiv, Ukraine*

Abstract

A novel method for parametric synthesis of an optimal controller, grounded in variational calculus, has been developed, assuming system mathematical model is expressed by a differential equation in operator form, with both sides articulated as algebraic polynomials in variable p=d/dt. The mathematical model of the controller is represented in a similar manner. An Euler-Poisson equation system for the extremal variational problem was derived, leading to an analytical expression for determining the settings for the specified controller structure by equating polynomial coefficients from the optimization task with those from the original system and controller equations. A computer experiment involving neural network implementation of this parametric synthesis method demonstrated high effectiveness, with accuracy reaching 99.3% and losses not exceeding 0.5%. These results confirm the superior performance of the neural network model in prediction accuracy and error minimization compared to traditional methods. ROC analysis of the neural network controller, neuro-fuzzy controller, and "classical" PID controller showed that both neural network and neuro-fuzzy controllers achieved high accuracy with minimal false positives, underscoring their reliability in precision-critical applications. Conversely, cubic spline interpolation and the "classical" PID controller displayed lower accuracy and higher false positives, emphasizing the advanced control methods' advantages for complex systems.

Keywords

optimal controller, parametric synthesis, dynamic system, control object, neural network, helicopter turboshaft engine, gas-generator rotor r.p.m.

✉ victoria.a.vysotska@lpnu.ua (V. Vysotska); vasyl.v.lytvyn@lpnu.ua (V. Lytvyn); serhii.vladov@univd.edu.ua (S. Vladov); klk.vonrgp@gmail.com (V. Vasylenko); krishan@ki-maup.com.ua (O. Kryshan)

🆔 0000-0001-6417-3689 (V. Vysotska); 0000-0002-9676-0180 (V. Lytvyn); 0000-0001-8009-5254 (S. Vladov); 0000-0002-9313-861X (V. Vasylenko); 0000-0002-2967-0126 (O. Kryshan)

1. Introduction

The parametric synthesis of optimal controllers for dynamic systems represents a critical challenge in control theory, particularly when aiming to achieve desired system performance under varying operational conditions [1–3]. This research leverages the principles of variational calculus to develop a general mathematical model for dynamic systems, enabling the precise formulation and solution of optimization problems associated with controller design [4, 5]. By systematically deriving the optimal control parameters, this approach ensures enhanced system stability, performance, and adaptability, making it a robust framework for the controllers' synthesis in complex dynamic environments [6].

The need for highly effective methods to synthesize optimal control parameters for dynamic systems is driven by increasing complexity and demands in modern technical systems. With growing variability in external influences and uncertainty in dynamic processes, ensuring stability and performance in controlled systems is crucial. Variational calculus enables enhanced adaptability, precision, and stability across a wide range of operating conditions, making it particularly relevant for fields such as aviation [7], energy [8], and robotics [9].

2. Related works

Research in the field of optimal controller parametric synthesis using variational calculus for dynamic systems has evolved over several decades, with foundational researches establishing the core principles. Initial research focused on applying variational techniques to derive optimal control laws for both linear and nonlinear dynamic systems. These early efforts demonstrated the potential for variational calculus to achieve precise control parameterization, leading to significant improvements in system stability and performance [10, 11]. Researchers successfully applied these methods to relatively simple systems, paving the way for more complex applications [12, 13].

As the field progressed, researchers began to address the challenges associated with real-world dynamic systems, including nonlinearity, time-varying parameters, and external disturbances [14, 15]. Researches explored the variational calculus extension to more sophisticated dynamic models, incorporating constraints such as actuator limitations, time delays, and uncertainties [16, 17]. This phase of research highlighted the versatility and robustness of variational calculus in handling complex dynamic behaviors, making it applicable to a wide range of engineering systems [18, 19]. Advances in computational methods also played a critical role during this period, enabling more efficient implementation of variational techniques for optimal controller synthesis [20].

In recent years, the variational calculus with modern optimization algorithms integration has led to further enhancements in the synthesis process. Researchers have combined these methods with gradient-based optimization, evolutionary algorithms, and machine learning techniques to address multi-dimensional and multi-agent systems [21–23]. These innovations have expanded the applicability of variational calculus to more complex scenarios, such as aerospace systems [24], robotics [25], and large-scale industrial processes [26]. Current research continues to explore new avenues for optimizing controller parameters, focusing on improving adaptability, computational efficiency, and real-time implementation in dynamic environments.

The necessity for parametric synthesis of controllers using variational calculus arises from the need to optimize control laws in complex dynamic systems, ensuring enhanced stability, adaptability, and performance across diverse operational scenarios.

3. Proposed technique

Based on [26, 27], it is assumed that the mathematical model describing the control object is represented by a differential equation in operator form with the right-hand side defined by the nominal value of the variable $p = \dfrac{d}{dt}$:

$$\underbrace{\left(p^n + d_{n-1} \cdot p^{n-1} + \ldots + d_1 \cdot p + d_0\right)}_{d(p)} \cdot y = \underbrace{\left(b_x \cdot p^x + b_{x-1} \cdot p^{x-1} + \ldots + b_1 \cdot p + b_0\right)}_{b(p)} \tag{1}$$

in this case $n > x$; $d(p)y = b(p)u$. The controller mathematical model is also presented in general form as:

$$\underbrace{\left(g_{x-1} \cdot p^{x-1} + \ldots + g_1 \cdot p + g_0\right)}_{g(p)} \cdot u = \underbrace{\left(r_1 + r_2 \cdot p + \ldots + r_n \cdot p^{n-1}\right)}_{r(p)} \tag{2}$$

in this case $g(p)u = r(p)y$.

As a quality functional, the integral-quadratic criterion is adopted in a generalized form, taking into account the constraint on energy costs for control [28] in the form:

$$J = \int_0^\infty \left(\sum_{i=1}^y q_{ii} \cdot y^{2 \cdot (i-1)} + u^2 \right) dt . \tag{3}$$

It is required to the controller structure (2) and the settings r_j determine such that the functional (3) reaches its minimum value. The controller structure is defined by r_j values that are non-zero, zero, or close to zero. To solve the optimization task [26, 28, 29], i.e., to determine the transient response to a disturbance given by non-zero initial conditions $y(0) = y_{10}$, $y'(0) = y_{20}$, ... $y^{(n)}(0) = y_{n0}$, while considering boundary conditions that ensure asymptotic stability:

$$y(t \to \infty) = y'(t \to \infty) = \ldots = y^{(n)}(t \to \infty) = 0. \tag{4}$$

Based on [26, 30, 31], the Lagrange function [32] is introduced. Since the constraints in this case are represented by a differential equation: $d(p)y = b(p)u$, the Lagrange multiplier λ should be replaced by a time-dependent Lagrange variable $\lambda(t)$ in the Lagrange function. Thus, the Lagrange function is expressed as:

$$L = \sum_{i=1}^y q_{ii} \cdot y^{2 \cdot (i-1)} + u^2 + \lambda(t) \cdot \left(d(p)^y - b(p)^u \right) . \tag{5}$$

Let us compose the Euler-Poisson equation for the functional $L(y, u)$ of two functions $y(t)$ and $u(t)$ and obtain a system of two equations:

$$\begin{cases} \dfrac{\partial L}{\partial y}-\dfrac{d}{dt}\cdot\dfrac{\partial L}{\partial y'}+\ldots(-1)^{\beta}\cdot\dfrac{d}{dt^{\beta}}\cdot\dfrac{\partial L}{\partial y^{(\beta)}}=d(-p)\lambda+2\cdot q\cdot(p^2)\cdot y=0 \\ \quad\dfrac{\partial L}{\partial u}-\dfrac{d}{dt}\cdot\dfrac{\partial L}{\partial u'}+\ldots(-1)^{\alpha}\cdot\dfrac{d}{dt^{\alpha}}\cdot\dfrac{\partial L}{\partial u^{(\alpha)}}=2\cdot u-b(-p)\lambda=0 \end{cases} \tag{6}$$

where $q\left(p^2\right)=\sum\limits_{i=1}^{\gamma} q_{ii}\cdot y^{2\cdot(i-1)}\cdot(-1)^{(i-1)}$.

By eliminating the variables u and λ from these equations, the equation for the variational task extremals has been obtained.

$$\left(d(p)\cdot d(-p)+b(p)\cdot b(-p)\cdot q\left(p^2\right)\right)y=0. \tag{7}$$

Characteristic polynomial

$$\Delta(p)=d(p)\cdot d(-p)+b(p)\cdot b(-p)\cdot q\left(p^2\right) \tag{8}$$

is an equation of degree $2\cdot\beta$, where $\beta=max\left\{n,(\gamma+x-1)\right\}$.

For simplicity, let $x + \gamma - 1 \le n$. This is a polynomial of even degrees P, which can be expressed in factored form:

$$\Delta(p)=\overline{\delta(p)}\cdot\overline{\delta(-p)}, \tag{9}$$

where $\overline{\delta(p)}$ is the polynomial of degree β containing the roots of a polynomial Δp with a negative real part.

On the other hand, the closed-loop system characteristic polynomial is given by:

$$D(p)=d(p)\cdot q(p)+b(p)\cdot r(p). \tag{10}$$

We form the identities $\overline{\delta(p)} = D(p)$ and compare the same degrees coefficients of P in these identities, resulting in equations for determining the desired controller settings.

To summarize, the formula for the optimal control $u(t)$ is obtained by solving the resulting polynomial equations and substituting the values back into the control law:

$$u(t)=\frac{r(p)}{g(p)}\cdot y(t). \tag{11}$$

where the coefficients r_j are determined from:

$$\Delta(p)=D(p). \tag{12}$$

Thus, solving these equations will provide the optimal controller settings and structure. This mathematical model presents a novel approach to optimizing dynamic systems control through several key aspects:

1. The model utilizes polynomials in the frequency domain to describe system and controller dynamics. This enables efficient optimization by considering both nominal system parameters and controller parameters.
2. Employing time-dependent Lagrange multipliers $\lambda(t)$ to account for control constraints provides flexibility in solving optimization problems and allows integration of stability conditions and energy expenditure constraints.
3. The introduction of an integral-quadratic criterion (quality criterion) allows for consideration of both dynamic system error and control costs, ensuring a more comprehensive and accurate analysis of control quality.
4. Introducing the characteristic polynomial $\Delta(p)$ and its factorization simplifies the optimal controller settings determination, streamlining the solution and interpretation process.

Optimal control $u(t)$ can be obtained by solving the characteristic polynomial equation and substituting the derived coefficients into the control expression. Solving these equations and substituting values yields optimal settings for r_j, minimizing functional $\mathcal{J}$ and satisfying all stability conditions. This ensures optimal system control considering given constraints and requirements.

Thus, the proposed model and method for optimal control represent an innovative approach to controlling dynamic systems, integrating modern polynomial analysis and Lagrange multipliers to achieve optimal outcomes.

4. Experiment

The work presents a computer experiment involving the proposed technique application in the helicopter turboshaft engines (TE) gas-generator rotor r.p.m. n_{TC} controlling task. The proposed neural network (Figure 1) is a tool for implementing the developed technique and is implemented using the TensorFlow and Keras libraries [33, 34].
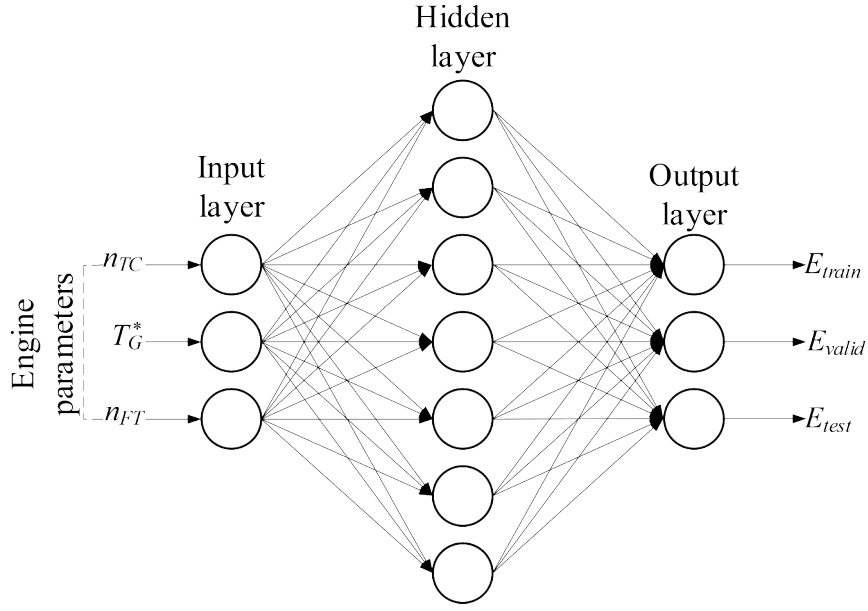
Figure 1: The proposed neural network (author's research).

The input layer takes four input parameters: the current gas-generator rotor r.p.m. n_{TC}, the gas temperature in front of the compressor turbine T_G^i, the engine inlet pressure P_i^i, and the fuel consumption G_T [35, 36], that is:

$$x = \left[n_{TC}, T_G^i, P_i^i, G_T \right]. \tag{13}$$

Hidden layers with ReLU activation function allow the model to capture nonlinear dependencies between input and output data.

The first hidden layer is defined as:

$$h_1 = ReLU \left(W_1 \cdot x + b_1 \right), \tag{14}$$

where W_1 is the first hidden layer weight matrix, b_1 is the first hidden layer bias, and ReLU is the ReLU activation function. A modified Smooth ReLU function described in [37] can be used, which preserves the ReLU advantages, such as the gradient absence for positive values, while adding smoothness for negative values.

The second hidden layer is defined as:

$$h_2 = ReLU \left(W_2 \cdot h_1 + b_2 \right), \tag{15}$$

where W_2 is the second hidden layer weight matrix, b_2 is the second hidden layer bias.

The output layer returns the desired gas-generator rotor r.p.m. n_{TC} predicted value, i.e.:

$$y = W_3 \cdot h_2 + b_3, \tag{16}$$

where W_3 is the output hidden layer weight matrix, b_2 is the output hidden layer bias.

A loss function is used to minimize the mean squared error (MSE), allowing the model to train from the difference between the predicted and actual gas-generator rotor r.p.m. n_{TC} values.

5. Results

The focus of this research is the TV3-117 TE, an integral component of the Mi-8MTV helicopter's propulsion system and its variants, extensively utilized in civil and military aviation [35–38]. Flight tests provided the gas-generator rotor r.p.m. n_{TC}, the gas temperature in front of the compressor turbine T_G^{ι}, the engine inlet pressure P_{ι}^{ι}, and the fuel consumption G_T, which formed a training dataset with 256 values for each parameter (Table 1).

Table 1
The training dataset fragment

Number	The gas-generator rotor r.p.m. n_{TC}	The gas temperature in front of the compressor turbine T_G^{ι},	The engine inlet pressure P_{ι}^{ι}	The fuel consumption G_T
1	0.973	0.961	0.983	0.973
...	...	...	...	...
42	0.983	0.966	0.988	0.977
...	...	...	...	...
139	0.988	0.950	0.992	0.970
...	...	...	...	...
256	0.985	0.952	0.984	0.971

The training dataset homogeneity assessment, detailed in [35–38], utilized Fisher-Pearson [39] and Fisher-Snedecor [40] criteria. According to these measures, the dataset is homogeneous, as the calculated Fisher-Pearson and Fisher-Snedecor values are below their respective critical thresholds, specifically $\chi^2=5.717<\chi^2_{critical}=6.6$ and $F=2.221<F_{critical}=2.58$. To evaluate the representativeness of the dataset, cluster analysis was performed using k-means [41, 42]. The dataset was split into training and test subsets in a 2:1 ratio (67 and 33 %, equating to 172 and 84 samples, respectively). The cluster analysis (Table 1) revealed eight distinct classes (I...VIII), confirming these groups presence and demonstrating consistency between the training and test datasets (Figure 2). These findings facilitated the optimal sample datasets determination: the training dataset comprises 256 elements (100 %), the validation dataset includes 172 elements (67 % of the training set), and the test dataset includes 84 elements (33 % of the training set).
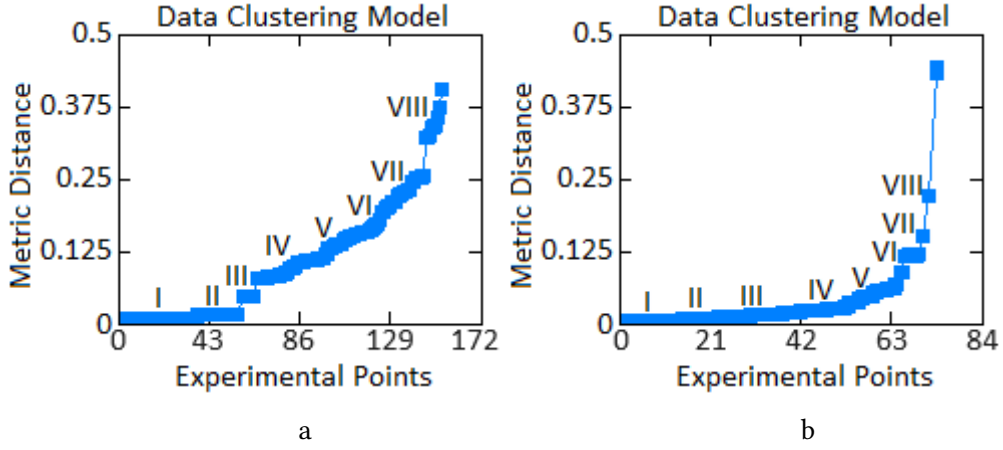
Figure 2: The cluster analysis results: a is the training dataset, b is the test (author's research).

During the neural network training initial phase, the epochs number impacts the *MSE*, calculated as [43]:

$$MSE_t = \frac{1}{N} \cdot \sum_{i=1}^{N} \left(\hat{n}_{TCi}^t - n_{TC} \right)^2,$$
(17)

where *N* represents the count observations (i.e., the elements number in the training dataset), n_{TCi} denotes the actual value, and $\hat{n}_{TCi}^t$ indicates the predicted value at training epoch *t*.

This is achieved by examining the MSE_t values at each epoch, as computed using (17), and evaluating the relations between MSE_t and the epochs number (Figure 3). Notably, the *MSE* metric in this research is influenced by the neural network's loss function, with the model error magnitude reflecting the difference between predicted and actual values.

To identify the neural network training epochs optimal number, a training curve is analyzed to pinpoint the epoch where the validation dataset error is minimized or reaches stability, indicating that further training yields no significant improvement. For each epoch $t \in [1, t]$, the *MSE* on the validation dataset $MSE_{val}(t)$ is calculated. The epochs optimal number t^* is determined as:

$$t^{\lower.5ex\hbox{ι}} = min \left\{ t \,\middle|\, \forall\, t^{'}, \left| MSE_{val}\left(t^{'}\right) - MSE_{val}\left(t^{'}\right) \right| \lower.5ex\hbox{ι} \epsilon \right\},$$
(18)

where t^* denotes the initial epoch from which the change in error on the validation dataset remains below the threshold value ϵ for all subsequent epochs.
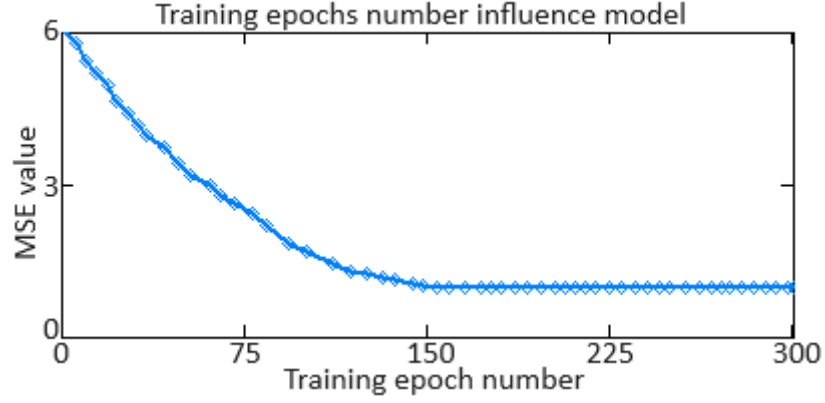
Figure 3: Diagram illustrating the epochs number impact on the mean squared error (author's research).

The findings suggest that 160 training epochs are adequate to reach the minimum value of MSE_{min} = 0.969.

To assess neural network performance during the subsequent stage of training, accuracy (Figure 4) and loss (Figure 5) are calculated over 160 training epochs. The Accuracy metric quantifies the proportion of correctly predicted values, whereas the Loss metric indicates the mean squared error of predictions, reflecting the extent of deviation from actual values.

To estimate the accurate calculations proportion for the gas-generator rotor r.p.m. n_{TC}, the Accuracy metric is employed (Figure 4), which is calculated at training epoch t using the following expression:

$$Accuracy_t = \frac{1}{N} \cdot \sum_{i=1}^{N} I\left(\hat{n}_{TCi}^t = n_{TC}\right),$$ (19)

where I represents an indicator function that equals 1 if the predicted value matches the true value, and 0 otherwise.

As illustrated in Figures 4 and 5, these metrics suggest that the neural network model achieves high accuracy (99.3 %) in predictions and demonstrates efficiency, as the mean squared error remains below 2.5 %. Additionally, a substantial decrease in the loss function from 2.5 to 0.5 % indicates an improvement in model quality throughout the training process.
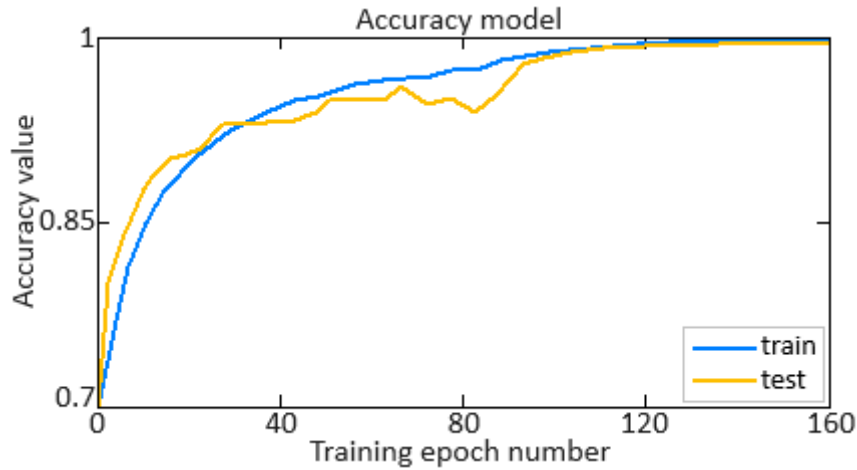
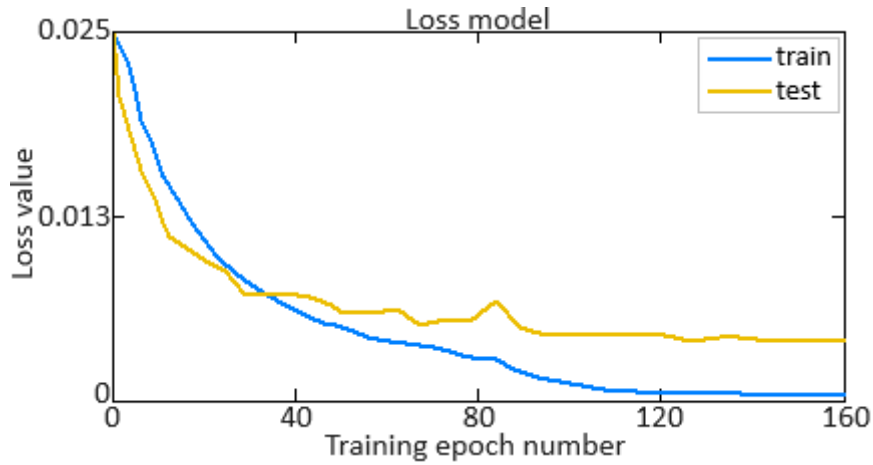**Figure 4:** The accuracy metric diagram (author's research).

Figure 5: The loss metric diagram (author's research).

Simulation results for the automatic control system of the gas-generator rotor r.p.m. n_{TC} using various PID controllers are shown in Figure 6. The neural network regulator is represented by a blue transient response, the neuro-fuzzy controller developed in [43] is depicted in black, and the "classical" PID controller [44] is shown in red.

The transient responses of the neural network and neuro-fuzzy controllers exhibit identical speed (transient process time of 1.5 seconds), which is notably shorter compared to the transient process time of 2.5 seconds observed with the "classical" controller.

In practice, the helicopter TE model is described by a high-order differential equation (up to the 30th order) [45]. This poses challenges in synthesizing controllers. Simplified models, typically described by the 2nd to 4th order equations, are used in the control systems development. However, not all controllers can ensure proper system performance under real flight conditions. Therefore, the helicopter TE various operating modes are considered in the control systems research and simulation.
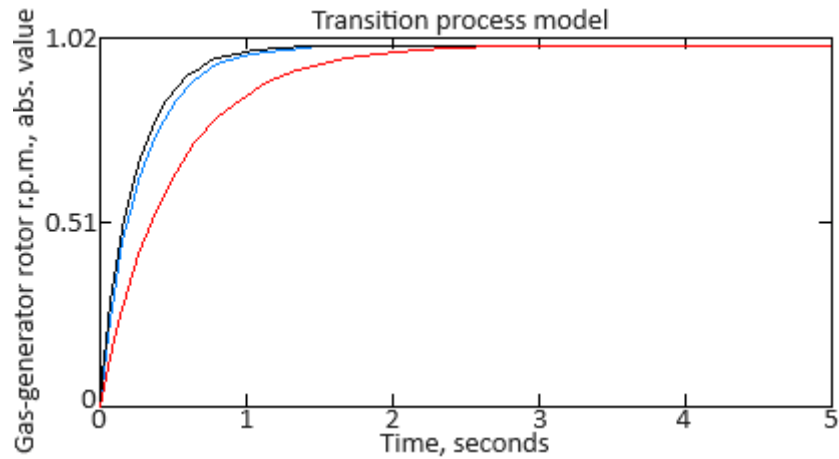
Figure 6: The diagrams of transient processes for the gas-generator rotor r.p.m. n_{TC} during engine operation in the helicopter turboshaft engines cruise mode (author's research).

The helicopter TE model presented in [35–38] is relevant for the cruising (primary) mode. The research also examines engine models in two additional modes: emergency (climbing) and idle (ground) conditions.

The gas-generator rotor r.p.m. n_{TC} transient characteristics with various PID controllers during the helicopter TE emergency operation are shown in Figure 7.
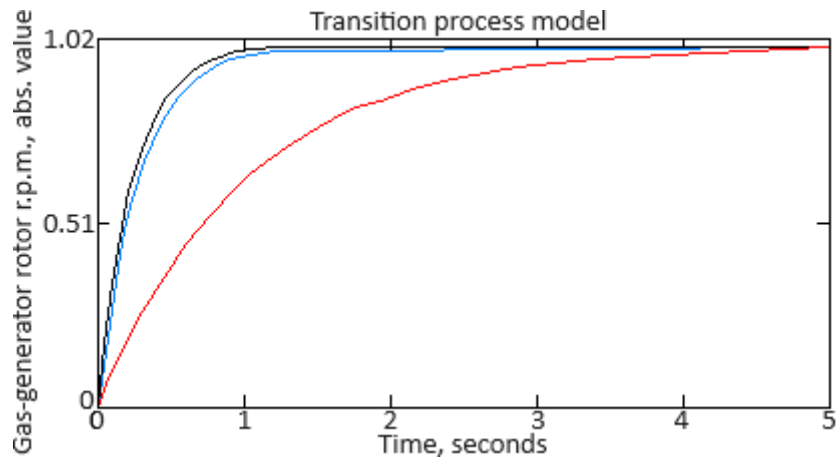

Figure 7: The diagrams illustrating the transient processes during helicopter turboshaft engines operation in climb mode (author's research).

Figure 8 shows the simulation results for the system in idle mode. In maximum operating conditions, both neural network and neuro-fuzzy PID controllers achieve a transient response time of 2 seconds. In contrast, the system with a classical controller has a transient response time of 6 seconds, significantly longer than with the neural network and neuro-fuzzy PID controllers. In idle mode, the system with the "classical" controller exhibits overshooting and oscillations, which are unacceptable. The neural network and neuro-fuzzy PID controllers achieve a transient response time of 1 second.
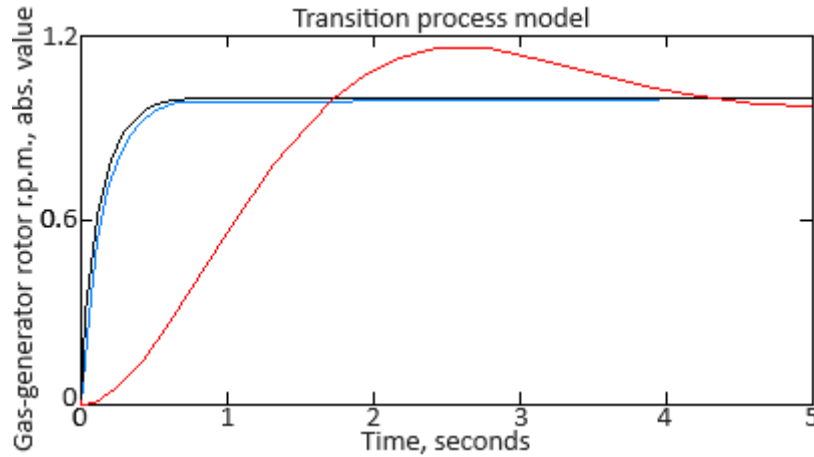
Figure 8: The diagrams illustrating the transient processes during helicopter turboshaft engines operation in ground mode (author's research).

6. Discussion

A method for parametric synthesis of an optimal controller based on variational calculus has been developed, assuming that the mathematical model of the system is represented by a differential equation in operator form, with both sides expressed as algebraic polynomials in the variable $p = \dfrac{d}{dt}$. The controller's mathematical model is similarly represented. Based on this, an Euler-Poisson equation system for the extremal variational task was derived. By equating the polynomials coefficients in the optimization task with those obtained from the system and the controller original equations, an analytical expression was obtained to determine the settings for the specified controller structure.

A computer experiment was conducted involving the neural network implementation of a parametric synthesis method for optimal control based on variational calculus (see Figure 1). The obtained results (accuracy up to 99.3 % as shown in Figure 3 and losses not exceeding 0.5 % as depicted in Figure 4) demonstrate the effectiveness and high precision of the developed neural network-based approach. These findings indicate that the neural network model achieves superior performance in terms of prediction accuracy and error minimization compared to traditional methods, validating its suitability for optimizing control systems in complex applications.

For ROC analysis across the three approaches (the proposed neural network controller, the neuro-fuzzy controller [43], and the "classical" PID controller [44]), true positive and false positive rates were computed for each class and method, followed by the generation of corresponding ROC curves. This process required establishing a binary classification for each class (distinguishing this class from all others).

A confusion matrix was constructed for the four classification categories (True Positives, True Negatives, False Positives, False Negatives). Each cell within the confusion matrix represents the frequency with which the actual class (rows) was predicted as the corresponding class (columns) for each method. For each class, True Positive Rate (TPR) and False Positive Rate (FPR) are calculated as [46–48]:

$$TPR = \frac{TP}{FP+TN}, FPR = \frac{FP}{FP+TN}. \tag{20}$$

The area under the ROC curve (AUC) can be approximated using the trapezoidal rule. Given that (TPR_i and FPR_i) represent the ROC curve points coordinates, the AUC is determined as [49–51]:

$$AUC = \sum_{i=1}^{P-1} \frac{TPR_i + TPR_{i+1}}{2} \cdot \left(FPR_{i+1} - FPR_i \right), \tag{21}$$

where P denotes the ROC curve points number [52]. The ROC analysis results are presented in Table 2.

Table 5
ROC analysis results (author's research)

Actual \ Predicted	The proposed neural network controller	The neuro-fuzzy controller [43]	The "classical" PID controller [44]
True Positives	94	94	0
True Negatives	4	3	11
False Positives	269	270	280
False Negatives	23	22	110
TPR	0.832	0.832	0
FPR	0.012	0.012	0.426
AUC	0.856	0.857	0.214

As a result, the neural network controller proposed in this work, along with the neuro-fuzzy controller [43], provides high accuracy with a minimal level false positive. The use cubic spline interpolation, on the contrary, leads to low accuracy and the highest number false positives.

This highlights the effectiveness and reliability the neural network and neuro-fuzzy controllers in scenarios where precision is critical. Their ability to minimize false positives without sacrificing accuracy makes them superior choices for applications requiring robust and accurate control mechanisms. Conversely, the "classical" PID controller's [44] higher rate false positives underscore its limitations in achieving the desired accuracy. The significant contrast in AUC values further emphasizes the advantages these advanced control methods bring to the table, making them preferable options in complex and dynamic systems.

These findings suggest that the neural network and neuro-fuzzy controllers are not only more reliable but also more adaptable to varying conditions, ensuring stable performance across

different operational modes. In contrast, the "classical" PID controller's [44] limitations could lead to suboptimal decisions in critical scenarios, potentially compromising system safety and efficiency.

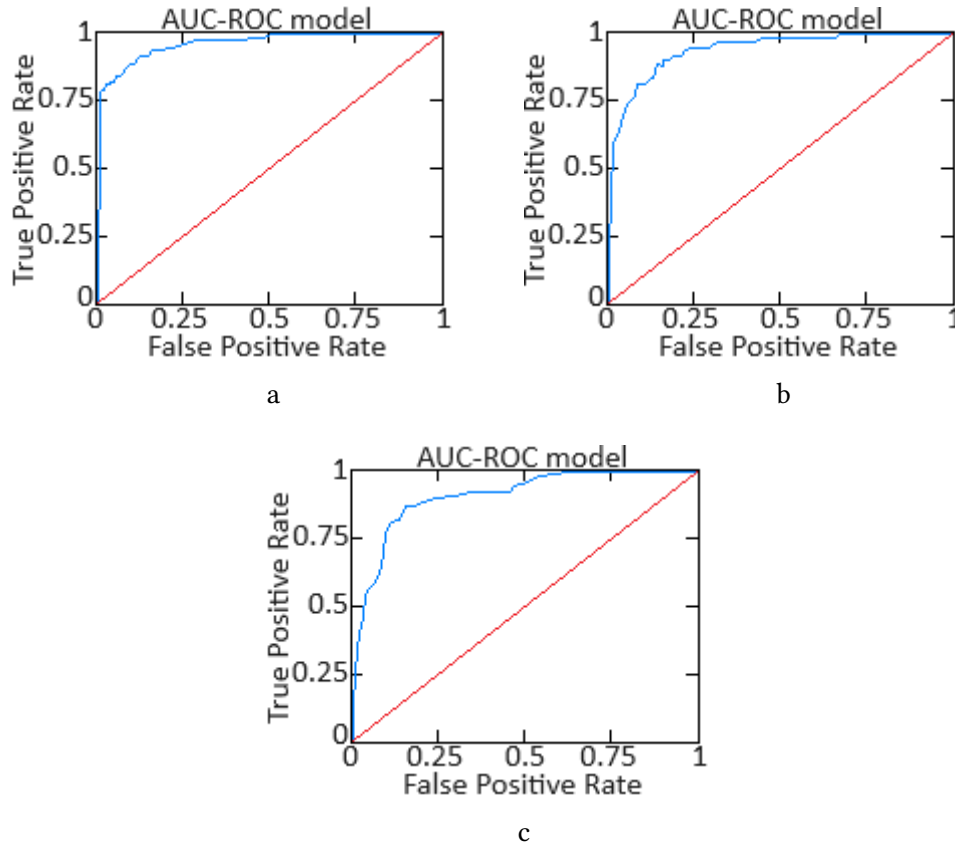The difference in the areas under the AUC curve is clearly illustrated in Figure 9.

a

b

c

Figure 9: The AUC-ROC curve: a is the proposed neural network controller; b is the neuro-fuzzy controller [43]; c is the "classical" PID controller [44] (author's research).

Future research in this domain should focus on several key areas to further enhance the developed method's applicability and robustness. One avenue is the extension of the parametric synthesis approach to multi-variable systems, where the interaction between multiple control variables can significantly impact overall system performance. Additionally, integrating advanced machine learning techniques, such as reinforcement learning or hybrid models combining neural networks with fuzzy logic, could further improve the controller's adaptability and precision in dynamic environments. Another promising direction involves real-time implementation and validation in practical applications, particularly in systems with high nonlinearity and uncertainty. This would not only confirm the theoretical results but also provide insights into potential modifications required for real-world deployment. Lastly, exploring the method's scalability and computational efficiency for larger, more complex systems could open new possibilities for its use in cutting-edge technologies, such as autonomous vehicles or advanced robotics.

7. Conclusions

This research scientific novelty lies in the development of a method for parametric synthesis of an optimal controller using variational calculus, with the system and controller models represented by differential equations in operator form as algebraic polynomials in the variable $p = \dfrac{d}{dt}$. This approach led to the derivation of an Euler-Poisson equation system for extremal variational tasks, providing an analytical expression for determining optimal controller settings. Furthermore, the implementation of this method through neural networks demonstrated remarkable accuracy, achieving prediction precision up to 99.3 % and minimal losses not exceeding 0.5 %. These results underscore the superiority of the proposed neural network-based approach in optimizing control systems, particularly in complex and dynamic applications, marking a significant advancement over traditional control methods.

The ROC analysis conducted for the three approaches is the proposed neural network controller, the neuro-fuzzy controller, and the "classical" PID controller is involved computing true positive and false positive rates for each class, followed by generating corresponding ROC curves based on binary classification for each class. The results demonstrated that both the neural network and neuro-fuzzy controllers achieved high accuracy with minimal false positives, highlighting their effectiveness and reliability in precision-critical scenarios. In contrast, cubic spline interpolation resulted in lower accuracy and the false positives highest number, while the "classical" PID controller exhibited limitations due to its higher rate of false positives. The marked difference in AUC values underscores the superiority of the neural network and neuro-fuzzy controllers, making them preferable for applications requiring robust and accurate control mechanisms in complex and dynamic systems.

Acknowledgements

References

[1]   D. Demin, Synthesis of optimal control of technological processes based on a multialternative parametric description of the final state, Eastern-European Journal of Enterprise Technologies 3:4 (87) (2017) 51–63. doi: 10.15587/1729-4061.2017.105294.

[2]   J. Huang, J. Wang, R. A. Ramirez-Mendoza, Synthesis of Optimal Controllers for Model Predictive Control, International Journal of Innovative Computing, Information and Control, 18:6 (2022) 1785–1798. doi: 10.24507/ijicic.18.06.1785.

[3]   M. Schütte, A. Eichler, H. Werner, Structured IQC Synthesis of Robust H2 Controllers in the Frequency Domain, IFAC-PapersOnLine 56:2 (2023) 10408–10413. doi: 10.1016/j.ifacol.2023.10.1055.

[4]   A. M. Borrell, V. Puig, O. Sename, Fixed-structure parameter-dependent state feedback controller: A scaled autonomous vehicle path-tracking application, Control Engineering Practice 147 (2024) 105911. doi: 10.1016/j.conengprac.2024.105911.

[5]   A. Didier, M. N. Zeilinger, Generalised Regret Optimal Controller Synthesis for Constrained Systems, IFAC-PapersOnLine 56:2 (2023) 2576–2582. doi: 10.1016/j.ifacol.2023.10.1341.

[6]   S. E. Vaca, D. Benítez, O. Camacho, Tuning equations for sliding mode controllers: An optimal multi-objective approach for non-minimum phase systems, Results in Engineering 23 (2024) 102695. doi: 10.1016/j.rineng.2024.102695.

[7]   S. Vladov, Y. Shmelov, R. Yakovliev, M. Petchenko, Neural Network Method for Parametric Adaptation Helicopters Turboshaft Engines On-Board Automatic Control System Parameters, CEUR Workshop Proceedings 3403 (2023) 179–195. URL: https://ceur-ws.org/Vol-3403/paper15.pdf

[8]   A. Silvestri, D. Coraci, S. Brandi, A. Capozzoli, E. Borkowski, J. Köhler, D. Wu, M. N. Zeilinger, A. Schlueter, Real building implementation of a deep reinforcement learning controller to enhance energy efficiency and indoor temperature control, Applied Energy 368 (2024) 123447. doi: 10.1016/j.apenergy.2024.123447.

[9]   D. Huang, Z. Xu, X. An, W. Wang, J. Xia, T. Meng, Precise control of magnetic soft microrobot in flowing environment, Sensors and Actuators A: Physical 369 (2024) 115155. doi: 10.1016/j.sna.2024.115155.

[10] Z. Ren, J. Lin, Z. Wu, S. Xie, Dynamic optimal control of flow front position in injection molding process: A control parameterization-based method, Journal of Process Control 132 (2023) 103125. doi: 10.1016/j.jprocont.2023.103125.

[11] R. Ortega, A. Bobtsov, N. Nikolaev, R. Costa-Castelló, Parameter estimation of two classes of nonlinear systems with non-separable nonlinear parameterizations, Automatica 163 (2024) 111559. doi: 10.1016/j.automatica.2024.111559.

[12] X. Ding, J. Xu, Z. Song, Y. Hou, Z. Shan, Trainable parameterized quantum encoding and application based on enhanced robustness and parallel computing, Chinese Journal of Physics 90 (2024) 901–910. doi: 10.1016/j.cjph.2024.05.044.

[13] H. Zhang, Y. Dai, C. Zhu, Region stability analysis and precise tracking control of linear stochastic systems, Applied Mathematics and Computation 465 (2024) 128402. doi: 10.1016/j.amc.2023.128402.

[14] H. Wang, J. Deng, L. Zhang, Q. Bao, Y. Mao, Enhanced disturbance observer-based hybrid cascade active disturbance rejection control design for high-precise tracking system in application to aerospace satellite, Aerospace Science and Technology 146 (2024). doi: 10.1016/j.ast.2024.108939.

[15] K. Liu, P. Yang, L. Jiao, R. Wang, Z. Yuan, S. Dong, Antisaturation fixed-time attitude tracking control based low-computation learning for uncertain quadrotor UAVs with external disturbances, Aerospace Science and Technology 142 (2023) 108668. doi: 10.1016/j.ast.2023.108668.

[16] Y. Huang, J. Liu, S. Zhu, F. Huang, Z. Chen, Robust Adaptive Control for Robotic System with External Disturbance and Guaranteed Parameter Estimation, IFAC-PapersOnLine 55:38 (2022) 178−183. doi: 10.1016/j.ifacol.2023.01.152.

[17] S. Wang, W. Jin, W. Chen, A novel payload swing control method based on active disturbance rejection control for 3D overhead crane systems with time-varying rope length, Journal of the Franklin Institute 361:6 (2024). doi: 10.1016/j.jfranklin.2024.106707.

[18] H. Miao, T. Song, J. Liu, J. Ye, Adaptive disturbance observer-based fast nonsingular terminal sliding mode control for quadrotors, Journal of the Franklin Institute 361:14 (2024) 107092. doi: 10.1016/j.jfranklin.2024.107092.

[19] D. Yan, Y. Liu, S. Zhang, B. Fang, F. Zhao, Z. Yang, PCNP: A RoCEv2 congestion control using precise CNP, Computer Networks 247 (2024) 110453. doi: 10.1016/j.comnet.2024.110453.

[20] J. H. Kim, T. Hagiwara, Kernel Approximation Approach to the L 1 Optimal Sampled-Data Controller Synthesis Problem, IFAC-PapersOnLine 50:1 (2017) 910−915. doi: 10.1016/j.ifacol.2017.08.086.

[21] F. M. Golmisheh, S. Shamaghdari, Heterogeneous optimal formation control of nonlinear multi-agent systems with unknown dynamics by safe reinforcement learning, Applied Mathematics and Computation 460 (2024) 128302. doi: 10.1016/j.amc.2023.128302.

[22] Z. Lin, J. Liu, C. L. P. Chen, G. Lai, Z. Wu, Z. Liu, Distributed fuzzy inverse optimal fixed-time control for uncertain multi-agent systems, Information Sciences 652 (2024) 119670. doi: 10.1016/j.ins.2023.119670.

[23] Y. Zhao, B. Niu, G. Zong, X. Zhao, K. H. Alharbi, Neural network-based adaptive optimal containment control for non-affine nonlinear multi-agent systems within an identifier-actor-critic framework, Journal of the Franklin Institute 360:12 (2023) 8118−8143. doi: 10.1016/j.jfranklin.2023.06.014.

[24] S. Vladov, R. Yakovliev, M. Bulakh, V. Vysotska, Neural Network Approximation of Helicopter Turboshaft Engine Parameters for Improved Efficiency, Energies 17:9 (2024) 2233. doi: 10.3390/en17092233.

[25] Y. Zheng, J. Zheng, K. Shao, H. Zhao, Z. Man, Z. Sun, Adaptive fuzzy sliding mode control of uncertain nonholonomic wheeled mobile robot with external disturbance and actuator saturation, Information Sciences 663 (2024) 120303. doi: 10.1016/j.ins.2024.120303.

[26] O. Nikulina, V. Severin, N. Kotsiuba, Parametric synthesis of control systems for the steam generator of a nuclear power plant, Eastern-European Journal of Enterprise Technologies 1:2 (115) (2022) 77−84. doi: 10.15587/1729-4061.2022.253126..

[27] A. Diveev, E. Shmalko, Adaptive Synthesized Control for Solving the Optimal Control Problem, Mathematics 11:19 (2023) 4035. doi: 10.3390/math11194035.

[28] S. Treanţă, O. M. Alsalami, Sufficient Efficiency Criteria for New Classes of Non-Convex Optimization Models, Axioms 13:9 (2024) 572. doi: 10.3390/axioms13090572.

[29] S. Dhahri and O. Naifar, Fault-Tolerant Tracking Control for Linear Parameter-Varying Systems under Actuator and Sensor Faults, Mathematics 11:23 (2023) 4738. doi: 10.3390/math11234738.

[30] A. Hauser et al., Valorizing Steelworks Gases by Coupling Novel Methane and Methanol Synthesis Reactors with an Economic Hybrid Model Predictive Controller, Metals, vol. 12:6 (2022) 1023. doi: 10.3390/met12061023.

[31] S. Stavrev, D. Ginchev, Reinforcement Learning Techniques in Optimizing Energy Systems, Electronics 13:8 (2024) 1459. doi: 10.3390/electronics13081459.

[32] Z. Gao, D. Li, D. Wang, Z. Yu, Lagrange Relaxation for the Capacitated Multi-Item Lot-Sizing Problem, Applied Sciences 14:15 (2024) 6517. doi: 10.3390/app14156517.

[33] L. Ferreira, G. Moreira, M. Hosseini, M. Lage, N. Ferreira, F. Miranda, Assessing the landscape of toolkits, frameworks, and authoring tools for urban visual analytics systems, Computers & Graphics 123 (2024) 104013. doi: 10.1016/j.cag.2024.104013.

[34] F. Zare, P. Mahmoudi-Nasr, R. Yousefpour, A real-time network based anomaly detection in industrial control systems, International Journal of Critical Infrastructure Protection 45 (2024) 100676. doi: 10.1016/j.ijcip.2024.100676.

[35] S. Vladov, L. Scislo, V. Sokurenko, O. Muzychuk, V. Vysotska, S. Osadchy, A. Sachenko, Neural Network Signal Integration from Thermogas-Dynamic Parameter Sensors for Helicopters Turboshaft Engines at Flight Operation Conditions, Sensors 24:13 (2024) 4246. doi: 10.3390/s24134246.

[36] S. Vladov, R. Yakovliev, V. Vysotska, M. Nazarkevych, V. Lytvyn, The Method of Restoring Lost Information from Sensors Based on Auto-Associative Neural Networks, Applied System Innovation 7:3 (2024) 53. doi: 10.3390/asi7030053.

[37] S. Vladov, R. Yakovliev, O. Hubachov, J. Rud, Y. Stushchanskyi, Neural Network Modeling of Helicopters Turboshaft Engines at Flight Modes Using an Approach Based on "Black Box" Models, CEUR Workshop Proceedings 3624 (2024) 116–135. URL: https://ceur-ws.org/Vol-3624/Paper_11.pdf

[38] S. Vladov, R. Yakovliev, O. Hubachov, J. Rud, Neuro-Fuzzy System for Detection Fuel Consumption of Helicopters Turboshaft Engines, CEUR Workshop Proceedings 3628 (2023) 55–72. URL: https://ceur-ws.org/Vol-3628/paper5.pdf

[39] H.-Y. Kim, Statistical notes for clinical researchers: Chi-squared test and Fisher's exact test, Restorative Dentistry & Endodontics 42:2 (2017) 152. doi: 10.5395/rde.2017.42.2.152.

[40] C. M. Stefanovic, A. G. Armada, X. Costa-Perez, Second Order Statistics of -Fisher-Snedecor Distribution and Their Application to Burst Error Rate Analysis of Multi-Hop Communications, IEEE Open Journal of the Communications Society 3 (2022) 2407–2424. doi: 10.1109/ojcoms.2022.3224835.

[41] S. Babichev, J. Krejci, J. Bicanek, V. Lytvynenko, Gene expression sequences clustering based on the internal and external clustering quality criteria. In Proceedings of the 2017 12th International Scientific and Technical Conference on Computer Sciences and Information Technologies (CSIT), Lviv, Ukraine, 05–08 September 2017. doi: 10.1109/STC-CSIT.2017.8098744.

[42] Z. Hu, E. Kashyap, O.K. Tyshchenko, GEOCLUS: A Fuzzy-Based Learning Algorithm for Clustering Expression Datasets. Lecture Notes on Data Engineering and Communications Technologies 134 (2022) 337–349. doi: 10.1007/978-3-031-04812-8_29.

[43] S. Vladov, L. Scislo, V. Sokurenko, O. Muzychuk, V. Vysotska, A. Sachenko, A. Yurko, Helicopter Turboshaft Engines' Gas Generator Rotor R.P.M. Neuro-Fuzzy On-Board Controller Development, Energies 17:16 (2024) 4033. doi: 10.3390/en17164033.

[44] E. Tsoutsanis, N. Meskin, Performance assessment of classical and fractional controllers for transient operation of gas turbine engines, IFAC-PapersOnLine 51:4 (2018) 687–692. doi: 10.1016/j.ifacol.2018.06.182.

[45] A. Sanfelici Bazanella, L. Campestrini, D. Eckhard, The data-driven approach to classical control theory, Annual Reviews in Control 56 (2023) 100906. doi: 10.1016/j.arcontrol.2023.100906.

[46] E. M. Cherrat, R. Alaoui, H. Bouzahir, Score fusion of finger vein and face for human recognition based on convolutional neural network model, International Journal of Computing 19:1 (2020) 11–19. doi: 10.47839/ijc.19.1.1688.

[47] A. R. Marakhimov, K. K. Khudaybergenov, Approach to the synthesis of neural network structure during classification, International Journal of Computing 19:1 (2020) 20–26. doi: 10.47839/ijc.19.1.1689.

[48] T. E. Romanova, P. I. Stetsyuk, A. M. Chugay, S. B. Shekhovtsov, Parallel Computing Technologies for Solving Optimization Problems of Geometric Design, Cybernetics and Systems Analysis 55:6 (2019) 894–904. doi: 10.1007/s10559-019-00199-4.

[49] V. V. Morozov, O. V. Kalnichenko, O. O. Mezentseva, The method of interaction modeling on basis of deep learning the neural networks in complex IT-projects, International Journal of Computing 19:1 (2020) 88–96. doi: 10.47839/ijc.19.1.1697.

[50] K. Andriushchenko, V. Rudyk, O. Riabchenko, M. Kachynska, N. Marynenko, L. Shergina, V. Kovtun, M. Tepliuk, A. Zhemba, O. Kuchai, Processes of managing information infrastructure of a digital enterprise in the framework of the «Industry 4.0» concept, Eastern-European Journal of Enterprise Technologies 1 (3–97) (2019) 60–72. doi: 10.15587/1729-4061.2019.157765.

[51] S. Vladov, Y. Shmelov, R. Yakovliev, Helicopters Aircraft Engines Self-Organizing Neural Network Automatic Control System, CEUR Workshop Proceedings 3137 (2022) 28–47. doi: 10.32782/cmis/3137-3.

[52] B. Rusyn, O. Lutsyk, R. Kosarevych, O. Kapshii, O. Karpin, T. Maksymyuk, J. Gazda, Rethinking Deep CNN Training: A Novel Approach for Quality-Aware Dataset Optimization, IEEE Access 12 (2024) 137427–137438. doi: 10.1109/access.2024.3414651.